CONTRIBUTIONS to SCIENCE, **3** (2): 167–180 (2006)
Institut d'Estudis Catalans, Barcelona

Dynamics of air pollution in the northwestern Mediterranean Basin (Catalonia) in summer using high-resolution air-quality modeling

José M. Baldasano[1*], Pedro Jiménez[1], Oriol Jorba[1], Eugeni López[1], René Parra[2] and Carlos Pérez[1]

1 Centro Nacional de Supercomputación (BSC-CNS). Earth Sciences División, Jordi Girona 29, 08034 Barcelona, Spain.

2 Currently at: Corporación para el mejoramiento de la Calidad del Aire de Quito (CORPAIRE)
Avenida Amazonas 29-25 e Inglaterra. Quito, Ecuador.

Resum

En la conca nord-oest del Mediterrani (NWMB) i Catalunya s'observa un complex comportament dels contaminants fotoquímics, condicionat, per una banda, per la superposició de circulacions atmosfèriques de diferents escales, i, per l'altra, pel patró d'emissions. Aquest treball combina els models MM5 (meteorològic), EMICAT2000 (d'emissions) i CMAQ (de transport químic), aplicats amb una resolució molt alta (1 h i 2 km) per analitzar l'elevada concentració de contaminants atmosfèrics fotoquímics sobre la regió NWMB (Catalunya) durant un episodi de contaminació fotoquímica característic del període estival: 13-16 d'agost de 2000. La combinació d'aquests models es mostra com una eina valuosa capaç de considerar l'ampli rang d'escales involucrades en els processos d'estudi. El treball se centra en els processos d'escala local, regional i sinòptica que controlen l'ozó troposfèric en la NWMB: fonts d'emissió importants i reaccions fotoquímiques complexes, transport advectiu i forta convecció, processos de deposició i intercanvi estratosfera-troposfera. En la troposfera baixa, les situacions amb recirculació de masses d'aire, juntament amb el complex patró d'emissions a Catalunya, són factors crítics en episodis de contaminació fotoquímica. La intensitat de la brisa de mar o el terral, els forçaments orogràfics tèrmics o mecànics en la complexa orografia del litoral poden provocar un transport vertical i una estratificació de contaminants atmosfèrics. Aquests fenòmens poden ser capturats gràcies a les simulacions que cobreixen tota la península Ibèrica (amb 1 h i 24 km de resolució).

Paraules clau: Modelització de la qualitat de l'aire, models de transport químic, fotoquímica, ozó, dinàmica atmosfèrica

Abstract

The complex behavior of photochemical pollutants in the northwestern Mediterranean Basin (NWMB) and Catalonia is conditioned by the superposition of circulations on different scales and on the pattern of emissions. This work combines the models MM5 (meteorological), EMICAT2000 (emissions), and CMAQ (chemistry transport model), which have been applied with very high temporal and spatial resolution (1 h and 2 km) to analyze the high levels of photochemical air pollution over the NWMB (Catalonia) during a typical summertime episode, in this study, 13–16 August, 2000. This combination of models is shown to be well-suited to address the large range of scales involved. The study focuses on local as well as medium– and large-scale processes controlling tropospheric ozone in the NWMB, notably, emissions and photochemistry, convective and advective transport, deposition processes, and stratosphere-troposphere exchange. In the lower troposphere, local re-circulation systems are of key importance, together with the complex pattern of emissions in Catalonia. The strength of the land-sea breeze circulation, together with thermally or mechanically driven convection over the complex orography of the eastern Iberian coast, can induce vertical transport and the layering of air pollution. These phenomena can be captured by simulations carried out for the domain covering the entire Iberian Peninsula (with a 1 h and 24 km resolution).

Keywords: Air-quality modeling, chemistry transport models, photochemistry, ozone, atmospheric dynamics

Introduction

The high levels of photochemical pollutants in summer (especially ozone, O_3) over the northwestern Mediterranean Basin (NWMB) and, specifically Catalonia, influence both ecosystems and human health. The cloud-free conditions and high solar radiation intensity promote the photochemical build-up of O_3 and other pollutants (Lelieveld *et al.*, 2002), and measurements have shown high O_3 concentrations in this Mediterranean region (e.g. Ziomas *et al.*, 1998; Millán *et al.*, 2000; Dueñas *et al.*, 2002). According to Ribas and Peñuelas (2004), the European Union's thresholds for human and plant protection are exceeded in the NWMB on 54 and 297 days per year, respectively. Atmospheric

* Corresponding author: José M. Baldasano Centro Nacional de Supercomputación (CNS). Earth Sciences División. Jordi Girona 29. 08034 Barcelona, Catalonia, EU. Tel. 34 934011746. Fax: 34 93340255. E-mail: jose.baldasano@bsc.es

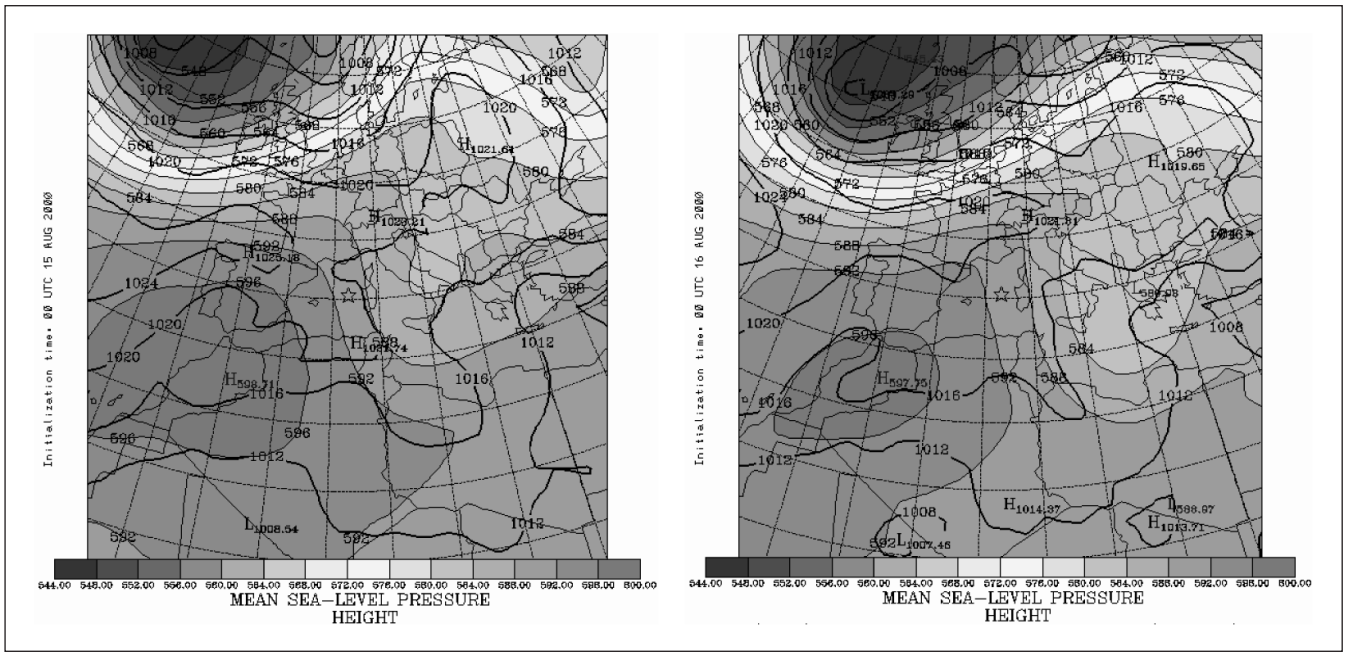

Figure 1. The northwestern Mediterranean Basin (NWMB, top); domain of Catalonia and topographical features in the area of study (center); and synoptic situation of 13–16 August, 2000 (contour map, 0000UTC surface analysis; shaded map, 0000UTC 500hPa analysis).

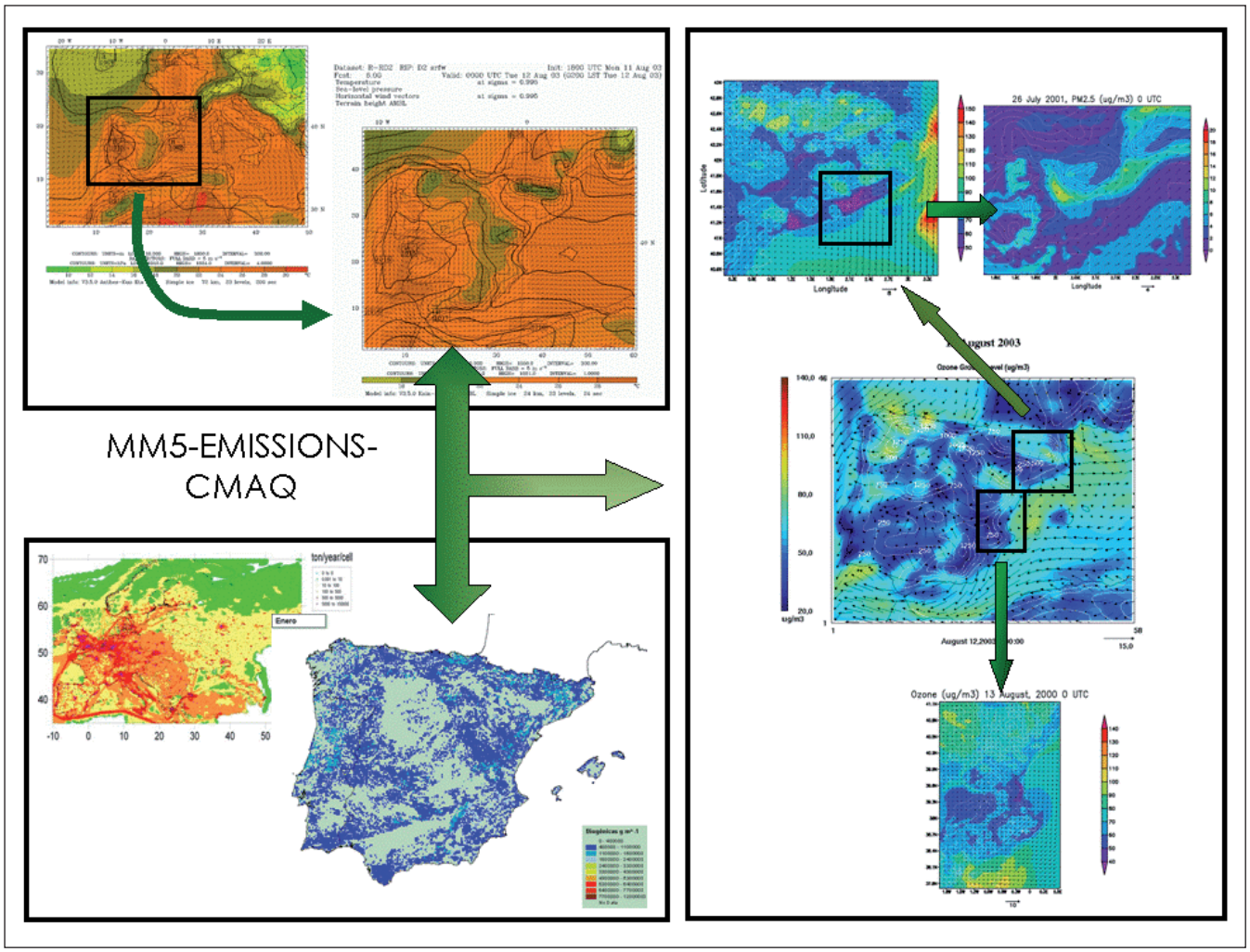

Figure 2. Structure of the model applied for photochemical simulations, combining MM5 meteorological model, emissions (EMEP, EMICAT2000, other inventories), and CMAQ chemical transport model.

chemistry transport model simulations suggest that summertime O_3 is enhanced in the entire Mediterranean troposphere, contributing substantially to the radiative forcing of the climate (Lawrence *et al.*, 1999; Hauglustaine and Brasseur, 2001).

The topography of the NWMB induces a complex flow regime associated with the development of mesoscale phenomena that interact with the synoptic flow (Baldasano *et al.*, 1994; Toll and Baldasano, 2000). Local orographic and land-sea breezes have important consequences for the dispersion of pollution emissions, especially during summer. The non-homogeneity of the terrain, the diverse land-use, and the different types of vegetation contribute to locally specific conditions. In fact, the flow structure is rather complicated because of the superposition of atmospheric circulations on a range of different scales. The aim of this work was to study the dynamics of physico-chemical processes in the NWMB (Catalonia) in order to explain the high levels of photochemical air pollution in this area during the summer. The period of 13-16 August, 2000, was selected to carry out the simulations, since it represented a weather pattern typical for this Mediterranean area in summer, during which pressure gradients are small (Fig. 1). Furthermore, this situation is representative of episodes of photochemical pollution in the NWMB, since these conditions dominate 45% of the annual and 78% of the summertime transport patterns over the area of study (Jorba *et al.*, 2004).

Methods

MM5-EMICAT2000-CMAQ

A summary of the structure of the models, which were applied with a high temporal and spatial resolution (1 h and 2 km for the domain of the NWMB), and the relationship among the different components is shown in Fig. 2.

The MM5 numerical weather prediction model (Dudhia, 1993) has been used in meteorological simulations. The MM5 options used for the simulations were: Mellor-Yamada scheme, as used in the Eta model for the planetary boundary layer (PBL) parameterization; Anthes-Kuo and Kain-Fritsch cumulus scheme; Dudhia simple ice moisture scheme; the cloud-radiation scheme; and the five-layer soil model. Initial and boundary conditions for the simulations were derived from a one-way nested simulation covering a domain of 1392 ? 1104 km^2 centered in the Iberian Peninsula (D1) with a spatial resolution of 24 km. Data were introduced using analysis data of the European Centre of Medium-Range Weather Forecasts (ECMWF) global model. Data were available at a 1-degree resolution (about 100 km at the NWMB latitude) at the standard pressure levels every 6 h.

The high-resolution (1 h and 1 km^2) EMICAT2000 emission model (Parra *et al.*, 2006) has been specifically developed and applied in Catalonia. Biogenic emissions were estimated using a methodology that takes into account local vegetation data (land-use distribution and biomass factors) and meteorological conditions (surface air temperature and solar radiation) together with emission factors for native Mediterranean species and cultures. On-road traffic emissions were estimated using the emission factors of the European model EMEP/CORINAIR–COPERTIII (Ntziachristos and Samaras, 2000) as a basis, and differencing the vehicle-park composition between weekdays and weekends (Jiménez *et al.*, 2005a). Levels of industrial emissions were derived from the records of several stacks monitored by the emissions network of the Environmental Department of the Catalonia Government (XEAC) and from the emissions of power stations, cement factories, refineries, olefins plants, chemical industries, and incinerators. A summary of the results is shown in Table 1, and a further description is provided in Sect. 3.

The chemical transport model used to compute the concentrations of photochemical pollutants for the period 13–16 August, 2000, was the CMAQ (Byun and Ching, 1999). The mother domain (D1) used EMEP emissions corresponding to the year 2000 (www.emep.int) for photochemical simulations. Based on the results of Jiménez *et al.* (2003), the chemical mechanism selected was CBM-IV (Gery *et al.*, 1989).

Ozone dynamics in the NWMB

In summer, the Mediterranean region is located between the Azorean high and Asian monsoon low-pressure regimes. The low troposphere and aloft layers are highly decoupled under those conditions. The low troposphere is dominated by mesoscale phenomena, while in the aloft layers (over 3000 m) the quasi-permanent weather system causes synoptically northwesterly flows over the Mediterranean. Although this flow is strongest and most persistent in August (Lelieveld *et al.*, 2002), during the NWMB episode of 13–16 August, 2000, the Azorean anticyclone dominated the weather over the Iberian Peninsula, with local very-low-pressure gradients. At the surface, a high-pressure ridge of about 1020 hPa penetrated over the NWMB. Within the anticyclone, subsidence contributed to the accumulation of air pollutants.

The backwards trajectories ending in the boundary layer and the lower troposphere (not shown) point to a local origin of air masses associated with re-circulation processes, common in the western Mediterranean Basin during summer (e.g. Baldasano *et al.*, 1994; Millán *et al.*, 1997; Jorba *et al.*, 2004; Pérez *et al.*, 2004). The back-trajectories at ground level indicate a regional recirculation regime over the Mediterranean Sea, while back-trajectories at 500 m are suggestive of transport from the Valencia-Castellón area, with a strong industrial influence. This pattern remains very similar up to an altitude of about 2.5 km. Therefore, during 13–16 August, 2000, photochemical pollution accumulated in the NWMB.

Figure 3 shows the diurnal O_3 patterns on 14 August, 2000. During night-time, the entire eastern Iberian coast was affected by down-slope winds from the mountains and generally offshore breezes. The Pyrenees and the French Central Massif channeled the northwesterly flow towards the Mediterranean Sea. Furthermore, the offshore wind drained the pollutants towards the coast through the river valleys. As the day advanced, a well-developed sea-breeze regime was established along the coast of the area, with circulation cells reaching up to 2 km in

Table 1. Summary of emissions by sources in Catalonia during the year 2000

	Primary air pollutants (kt year^{-1})						*Greenhouse gases (kt CO_2 eq year^{-1})*	
Source	*NO_x*	*NMVOC*	*CO*	*SO_2*	*TSP*	*Total (a)*	*(b)*	*(a)/(b) %*
1. Vegetation		46.9				46.9		
2. On-road traffic	62.4	49.5	259.0	1.3	15.7	387.9	8302.0	4.7
3. Industrial emissions	41.2	22.8	7.3	61.1	7.5	139.9	20361.0	0.7
Power generation	15.0	0.7	2.1	28.5	1.7	48.0	5698.0	0.8
Cement	9.6	0.3	3.5	1.4	4.2	19.0	8477.0	0.2
Oil refineries	8.5	6.4	1.1	25.0	0.9	41.9	2929.0	1.4
Olefins	2.9	2.4	0.0	6.2	0.7	12.2	690.0	1.8
Fugitives emissions		11.0				11.0		
Other	5.2	2.0	0.6	0.0	0.0	7.8	2567.0	0.3
4. Fossil-fuel use (residential and commercial)	3.3	0.2	1.1	2.3	0.3	7.2	3512.0	0.2
5. Use of solvents		17.2				17.2		
Total:	106.9	136.6	267.4	64.7	23.5	599.1	32175.0	1.9
%	17.84	22.80	44.64	10.80	3.92	100		
	Primary air pollutants (%)						*Greenhouse gases*	
Source	*NO_x*	*NMVOC*	*CO*	*SO_2*	*TSP*	*Total*	*%*	
1. Vegetation		34.33				7.83		
2. On-road traffic	58.37	36.24	96.86	2.01	66.81	64.75	25.80	
3. Industrial emissions	38.54	16.69	2.73	94.44	31.91	23.35	63.28	
Power generation	14.03	0.51	0.79	44.05	7.23	8.01	17.71	
Cement	8.98	0.22	1.31	2.16	17.87	3.17	26.35	
Oil refineries	7.95	4.69	0.41	38.64	3.83	6.99	9.10	
Olefins	2.71	1.76	0.00	9.58	2.98	2.04	2.14	
Fugitives emissions		8.05				1.84		
Other	4.86	1.46	0.22	0.00	0.00	1.30	7.98	
4. Fossil-fuel use (residential and commercial)	3.09	0.15	0.41	3.55	1.28	1.20	10.92	
5. Use of solvents		12.59				2.87		
Total:	100	100	100	100	100	100	100	

height, well above the PBL mixing height at about 800 m (Sicard *et al.*, 2006). After 08.00 UTC, onshore winds developed along the eastern Iberian coast, intensifying the anticyclonic circulation and deflecting the flow between the Pyrenees and the Central Massif toward the east.

The main emission sources in the domain of study are located at the coast, especially in the Barcelona urban area and the Tarragona industrial zone (Parra *et al.*, 2006). Biogenic sources are also of great importance near the Mediterranean coast, representing 34% of the total annual emission of volatile organic compounds (VOCs), especially since they contribute highly reactive compounds, such as aldehydes and isoprene. This percentage increases during summertime because of higher temperatures and solar radiation. Traffic emissions account for 58 and 36% of, respectively, the emissions of nitrogen oxides (NO_x) and VOCs, notably olefins and aromatic compounds. During summer, especially in August, traffic emissions increase due to the growing number of tourist vehicles during the peak holiday period. Therefore, at noon, air pollution from the Barcelona area and the road axis along the coast was transported land inward following the breeze front, arriving, e.g., at Plana de Vic (70 km downwind of Barcelona), where the flow decelerates, allowing O_3 and its precursors to accumulate, so that the European Union threshold O_3 level of 180 $\mu g\ m^{-3}$ was exceeded.

The industrial pole in the area of Tarragona plays a special role in concentrating an important amount of the industrial emissions. Furthermore, the domestic and commercial use of solvents represents 13% of VOCs emissions in the area (Parra *et al.*, 2006). The source of precursors attributable to the industrial sector in the domain of this study adds up to 41 Gg year^{-1} of NO_x and 23 Gg year^{-1} of VOCs. Annually, total emissions of O_3 precursors are 106.9 Gg year^{-1} of NO_x (58% traffic emissions; 39% industrial emissions) and 99.3 Gg year^{-1} of VOCs (34% biogenic emissions, 36% road traffic, 17% industrial emissions).

At the same time, in the southern part of the study area (Tarragona), during the morning the katabatic winds weaken and a clear land-sea breeze develops, associated with anabatic and valley winds, which transports pollutants emitted from the industrial area of Tarragona. The high O_3 concentrations in southern Catalonia are a consequence of the fact that

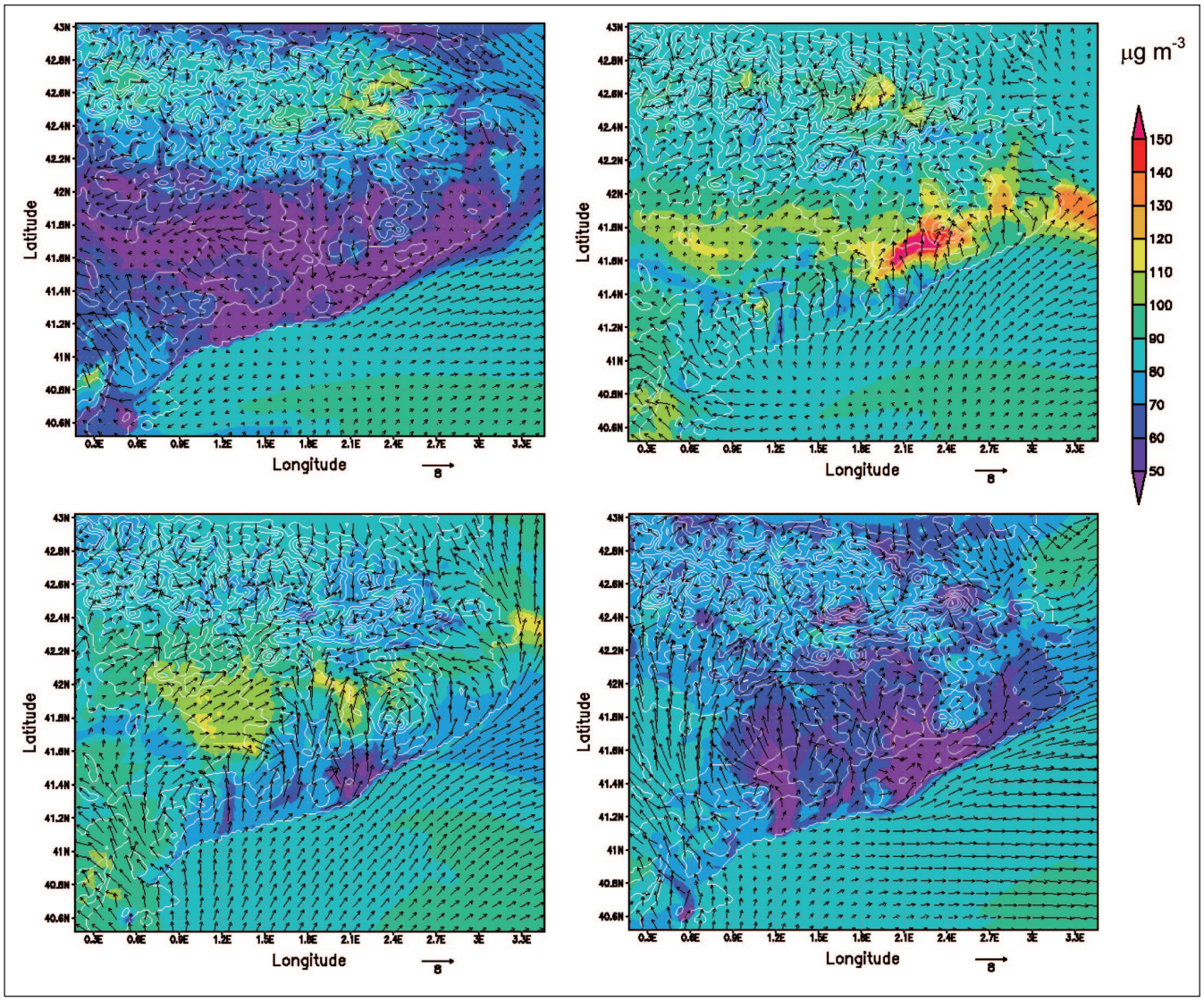

Figure 3. O_3 concentrations (µg m^{-3}) and wind fields (m s^{-1}) at ground-level over the NWMB calculated with MM5-EMICAT2000-CMAQ for 14 August, 2000, at 06.00UTC (top left), 12.00UTC (top right), 16.00UTC (bottom left), and 20.00UTC (bottom right).

the land-sea breeze is not sufficiently intense to overcome the littoral mountain range, allowing the accumulation of pollutants.

Land inward, over the central plateau, the flow is influenced by the presence of the pre-Pyrenees and the northwesterly wind aloft, allowing re-circulations that also promote the accumulation of O_3. This pattern persists during the afternoon although the breeze gains intensity and adds to the upslope winds, transporting pollutants over the pre-littoral mountain ranges. Around 19.00–20.00 UTC, the photochemical activity ceases, the sea-breeze regime loses intensity, and the coastal winds weaken. Inland, over the eastern part of the domain, strong southerly winds develop that dilute O_3. At night, land-inward winds calm with the development of a weak land breeze, with drainages in the valleys and katabatic winds. A larger-scale feature in the low troposphere is the flow canalization between the Pyrenees and the Central Massif, which introduces Atlantic air masses of northwesterly origin into the northeastern Iberian Peninsula region, as also concluded by Gangoiti *et al.* (2001). Simulations with MM5-EMICAT2000-CMAQ indicated that the concentration of photochemical air pollution in these Atlantic air masses is relatively low.

An important characteristic of the flow regime is that re-circulations arise from the orographic forcing. The strength of the land-sea breeze combines with the reinforcement of the complex orography along the eastern Iberian coast, causing a positive effect of upward vertical injection and layering of the air pollution. As the sea-breeze front advances inland, reaching the mountain ranges, the orographically induced injection can occur at different altitudes, with a subsequent return flow toward the coast (Fig. 4). Mechanical recirculation of air pollution typically occurs at Collserola Mountain (~500 m). At noon, the breeze usually reaches the first mountain chain, where it is reinforced by anabatic winds producing upward motions of up to 1.5–2 km altitude.

In the middle troposphere, the intense surface heating promotes the development of the Iberian thermal low (ITL) over the central part of the Iberian Peninsula (Millán *et al.*, 1996). The ITL also developed during the episode of 13–16 August, 2000, concurrent with the stagnant anticyclonic conditions. This

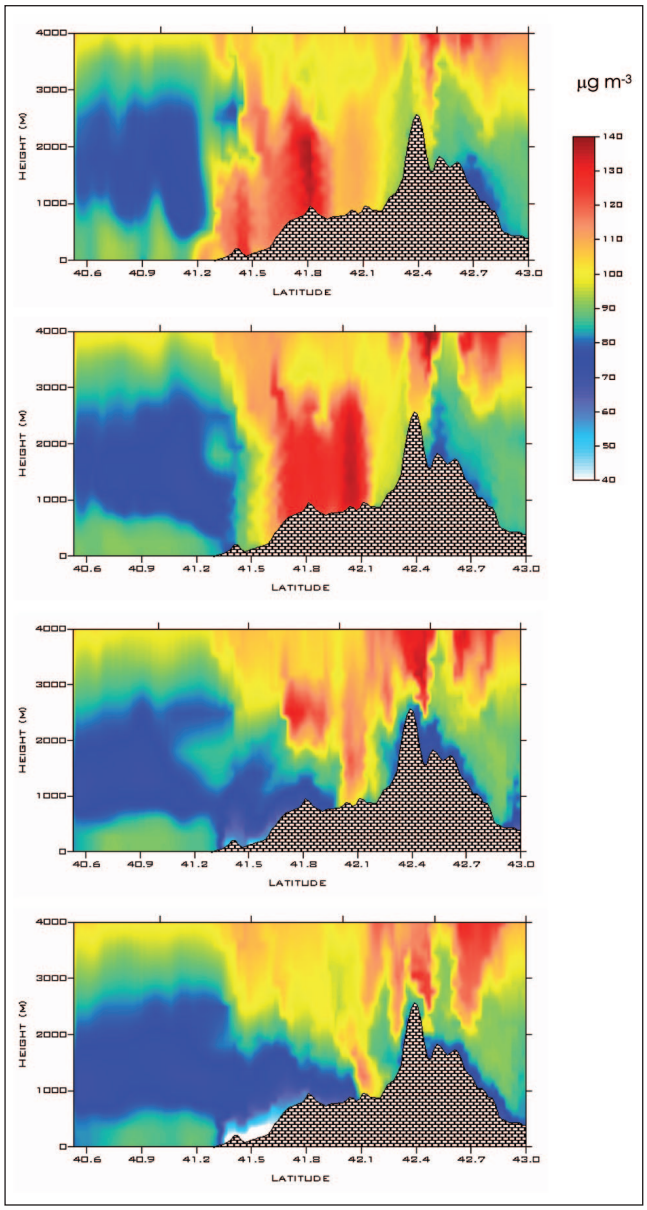

Figure 4. Recirculations over the northeastern Iberian Peninsula strongly influence O_3 (in µg m^{-3}) as calculated using MM5-EMICAT2000-CMAQ for 12.00, 14.00, 18.00, and 20.00 UTC, from top to bottom, respectively, for 14 August, 2000.

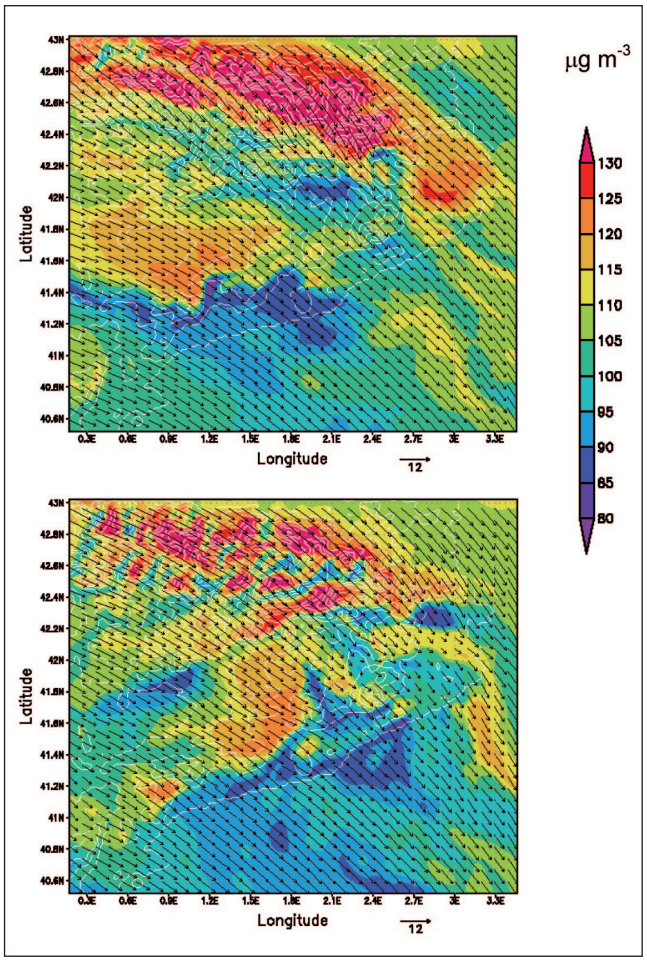

Figure 5. O_3 concentrations (µg m^{-3}) and wind fields (m s^{-1}) at 3500 m, 0600 UTC (top) and 1800 UTC (bottom) on 14 August, 2000, simulated for the NWMB with MM5-EMICAT2000-CMAQ.

peninsular-level ITL forces the convergence of surface winds from the coastal areas towards the central plateau, injecting polluted air masses into the middle troposphere. Once in this region, northwesterly winds transport pollutants within a stratified layer, indicating that air masses arriving in the NWMB have an Atlantic origin (Fig. 5). This middle-troposphere air of Atlantic origin collects anthropogenic pollutants as the air masses flow over the central Iberian Plateau. These air masses carry a relatively large amount of O_3 and precursor gases, injected by mid-level convective processes. In the middle troposphere, medium-range transport toward the Mediterranean coast takes place, as indicated by the simulations with MM5-EMICAT2000-CMAQ. At an altitude of 3–4 km, air masses with relatively high O_3 concentrations (>120 µg m^{-3}) are transported from the central plateau through the western boundary of the area of study at 06.00 UTC. The anticyclonic subsidence contributes to the accumulation of air pollution over the littoral mountain ranges at least until 18.00 UTC. Subsequently, the pollutants are transported towards the Mediterranean Sea, where they further subside, which also contributes to the stabilization and layering of air pollution. A fraction of these pollutants is advected out of the domain and the remainder is incorporated into the sea-breeze system during the following morning.

A summary of the dynamics of air pollutants is shown in Fig. 6 for ground-based and aloft pollution on a horizontal layer; and in Fig. 7 for the vertical dynamics of pollutants over the NWMB.

Results of MM5-EMICAT2000-CMAQ evaluation

Evaluation of the CMAQ chemical transport model

Keeping in mind that surface measurements produce a value only at a given horizontal location and height, while the concentration predicted by the model represents a volume-averaged value, we statistically evaluated the performance of the models by comparing the first-layer simulations results with the values measured in the meteorological and air-quality stations of the domain under study. The hourly data of air-quality

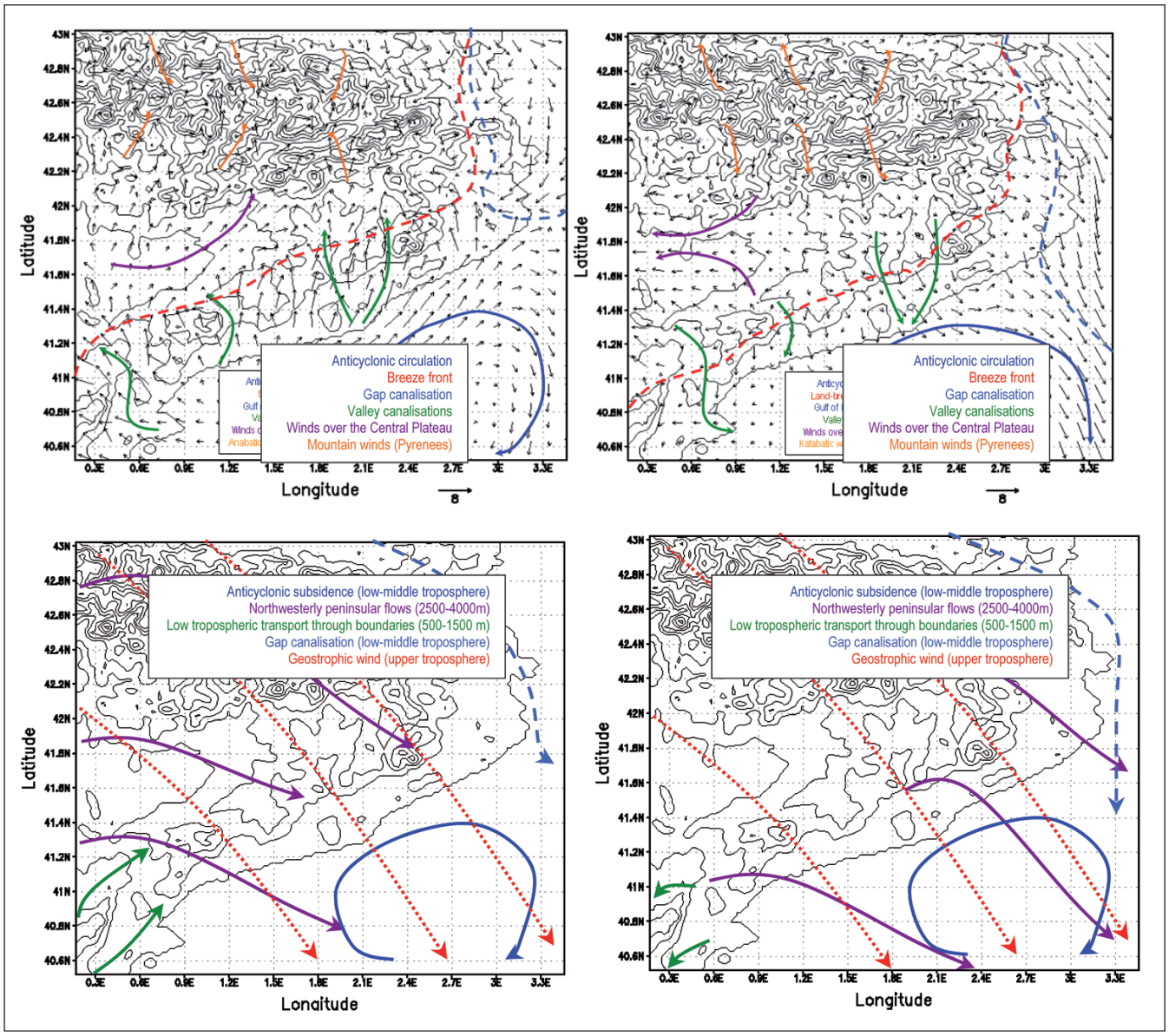

Figure 6. Conceptual representation of the flow regime during the day (left) and night (right) controlling near-surface air pollution (top) and the atmospheric dynamics aloft (bottom) over the NWMB during a typical summertime episode (13–16 August, 2000).

stations were averaged over the study domain and used to set the evaluation parameters. Hourly measures of ground-level O_3, NO_x, and carbon monoxide (CO) were provided by 48 air-quality surface stations belonging to the Environmental Department of the Government of Catalonia. European Directive 2002/3/EC states that with respect to O_3 in ambient air, there is an uncertainty of 50% regarding the air-quality objective for modeling assessment methods. In addition, the US Environmental Protection Agency has developed guidelines (USEPA, 1991) drawn from Tesche *et al.* (1990). Categorical statistics as derived from Kang *et al.* (2003; 2004) have also been used to evaluate the behavior of the model. Observation/prediction pairs were excluded from the analysis when the observed concentration was below a cut-off level of 120 μg m^{-3} (Hogrefe *et al.*, 2001). The statistical parameters used are defined in Table 2.

Day-to-day evaluation of ozone during the period 13–16 August, 2000

Table 3 shows the results of both the discrete and categorical statistical analysis detailed for each day of the episode of photochemical pollution of 13–16 August 2000. As an example, the results of the evaluation are shown for the station of Barcelona-Eixample (Fig. 8) and Vic (Fig. 9), located downwind from the city of Barcelona. The model results met the requirements for a discrete evaluation on all days of the episode. O_3 MNBE was negative on each day, ranging from –2.1% on the first day of simulation to –14.3% on August 15. That suggests a slight tendency towards underprediction; however, the USEPA goals of ±15% were achieved. This negative bias suggests that the chemistry of O_3 production may not be sufficiently reactive. The unpaired peak accuracy (UPA) was overestimated on the first and last days of the simulations (14.4 and 5.2%, respectively) and underestimated on the central days of the episode

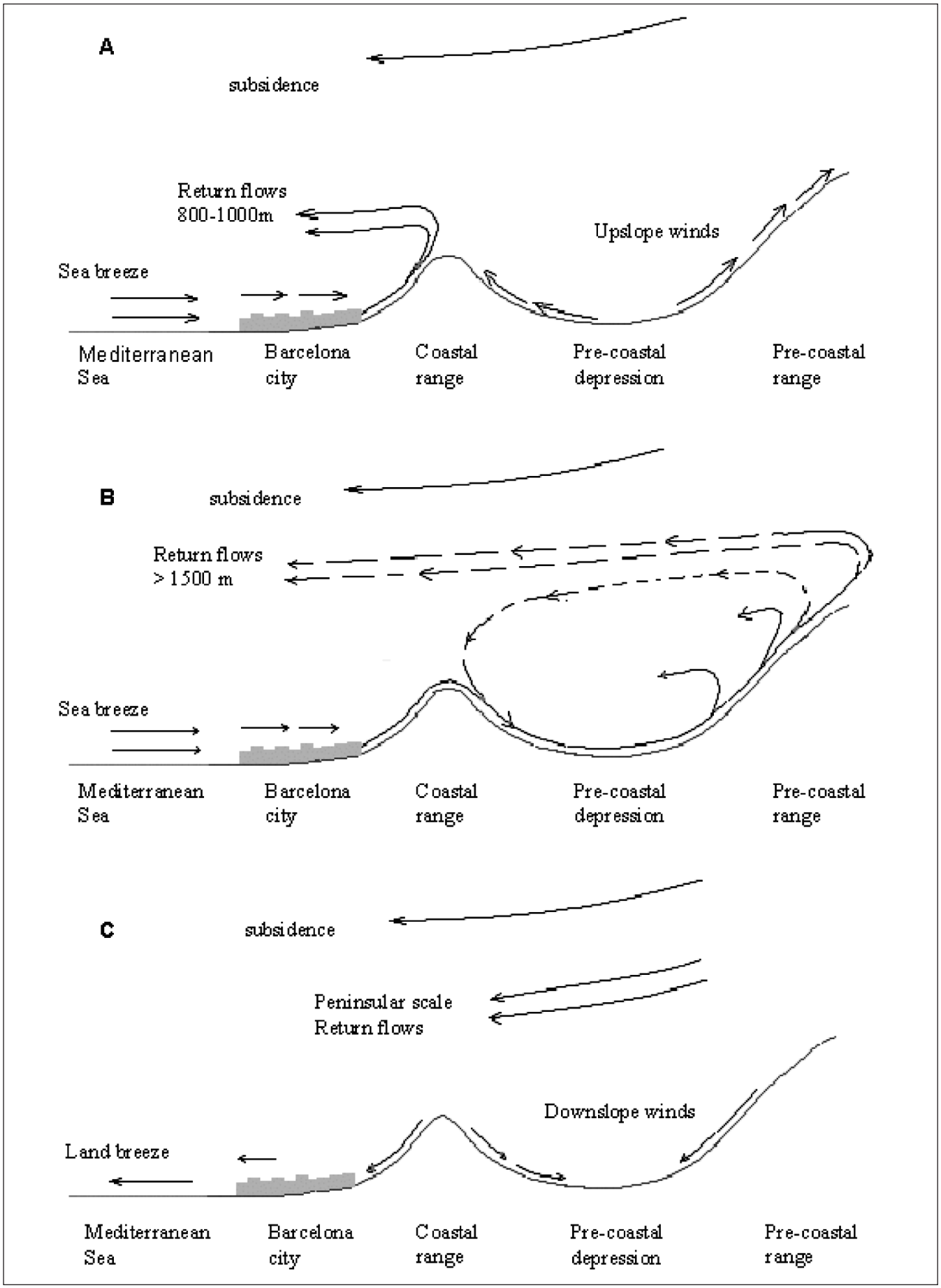

Figure 7. Vertical scheme of the dynamics of air pollutants over the NWMB for a profile including the Mediterranean Sea-city of Barcelona-coastal mountain range. A during the morning (up), at noon (center), and in the afternoon (down).

Table 2. Definition of statistic parameters used for model evaluation[a].

Discrete evaluation	
Mean bias (MB)	$MB = \frac{1}{N}\sum_{1}^{N}(Model - Obs)$
Mean normalized bias error (MNBE)	$MNBE = \frac{1}{N}\sum_{1}^{N}\left(\frac{(Model - Obs)}{Obs}\right)\cdot 100\%$
Mean fractionalized bias (MFB)	$MFB = \frac{1}{N}\sum_{1}^{N}\left(\frac{(Model - Obs)}{\left(\frac{Model + Obs}{2}\right)}\right)\cdot 100\%$
Mean absolute gross error (MAGE)	$MAGE = \frac{1}{N}\sum_{1}^{N}\lvert Model - Obs\rvert$
Mean normalized gross error (MNGE)	$MNGE = \frac{1}{N}\sum_{1}^{N}\left(\frac{\lvert Model - Obs\rvert}{Obs}\right)\cdot 100\%$
Normalized mean error (NME)	$NME = \frac{\sum_{1}^{N}\lvert Model - Obs\rvert}{\sum_{1}^{N}Obs}\cdot 100\%$
Normalized mean bias (NMB)	$NMB = \frac{\sum_{1}^{N}(Model - Obs)}{\sum_{1}^{N}(Obs)}\cdot 100\%$
Root mean square error (RMSE)	$RMSE = \sqrt{\frac{1}{N}\sum_{1}^{N}(Model - Obs)^2}$
Unpaired peak accuracy (UPA)	$UPA = \frac{Model_{max} - Obs_{max}}{Obs_{max}}\cdot 100\%$
Categorical Evaluation	
Accuracy (A)	$A = \left(\frac{b + c}{a + b + c + d}\right)\times 100\%$
Critical success index (CSI)	$CSI = \left(\frac{b}{a + b + d}\right)\times 100\%$
Probability of detection (POD)	$POD = \left(\frac{b}{b + d}\right)\times 100\%$
Bias (B)	$B = \left(\frac{a + b}{b + d}\right)$
False-alarm ratio (FAR)	$FAR = \left(\frac{a}{a + b}\right)\times 100\%$

[a] Model, modeled (data obtained from simulations); Obs, observations (ambient data); N, number of observations; a, forecast of an exceedance that did not occur; b, forecast of an exceedance that occurred; c, forecast of a non-exceedance that did not occur; d, non-forecast of an exceedance that occurred.

Table 3. Statistical measures of model performance for 1-h O3 during the episode of 13–16 August, 2000.

	EPA Goal	*August 13, 2000*	*August 14, 2000*	*August 15, 2000*	*August 16, 2000*
	Discrete evaluation				
Observed peak (μgm^{-3})		157	177	189	171
Modeled peak (μgm^{-3})		188	170	167	180
UPA (%)	<±20%	14.4	-3.8	-11.7	5.2
MNBE (%)	<±15%	-2.1	-11.0	-14.3	-5.6
MNGE (%)	<35%	16.8	19.8	21.7	26.7
	Categorical evaluation				
A (%)		91.1	92.2	90.0	89.7
B(%)		0.7	0.1	0.1	0.4
POD (%)		22.1	6.9	9.6	11.5
CSI(%)		15.0	6.7	9.2	9.1
FAR (%)		67.9	33.3	31.3	69.6

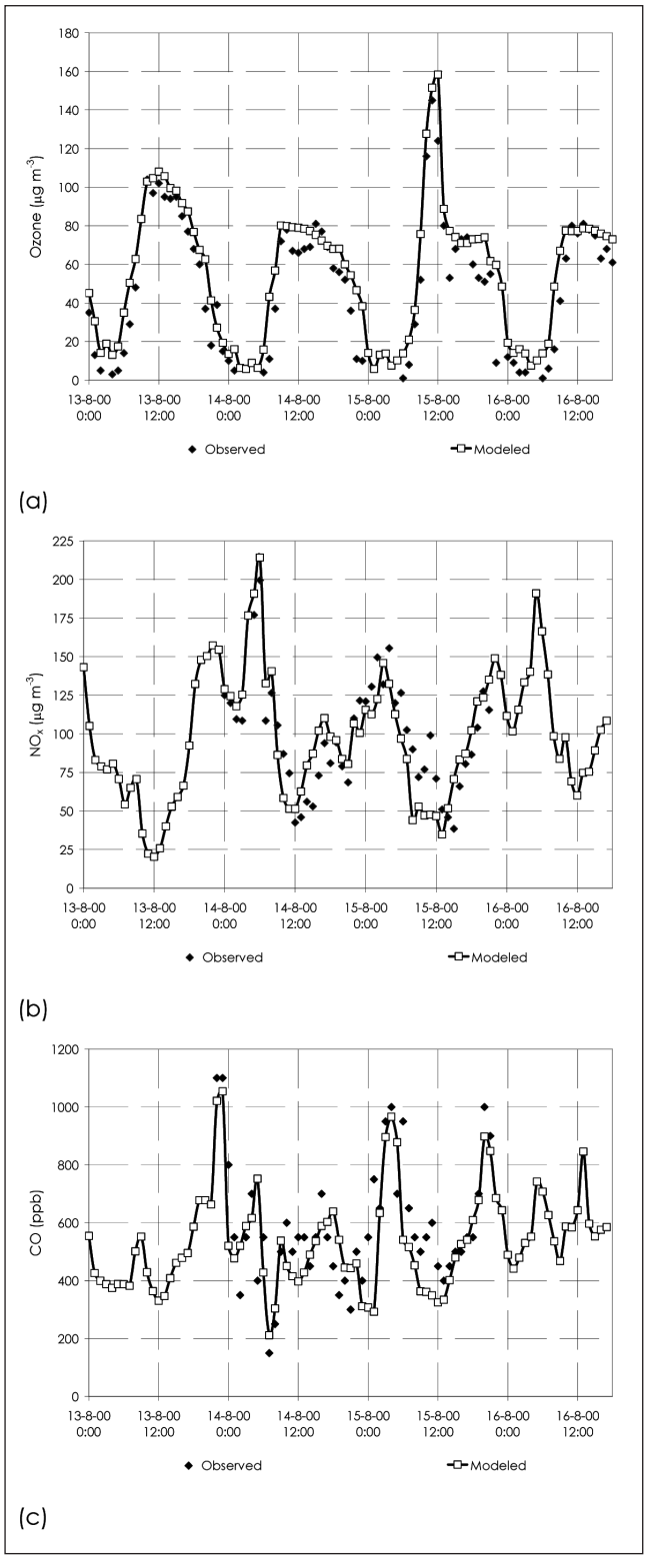

Figure 8. Time series for (a) ozone, (*b*) NO_x, and (c) CO for observations (black diamonds) and simulations (solid line, white squares) in the area of Barcelona for 13–16 August, 2000.

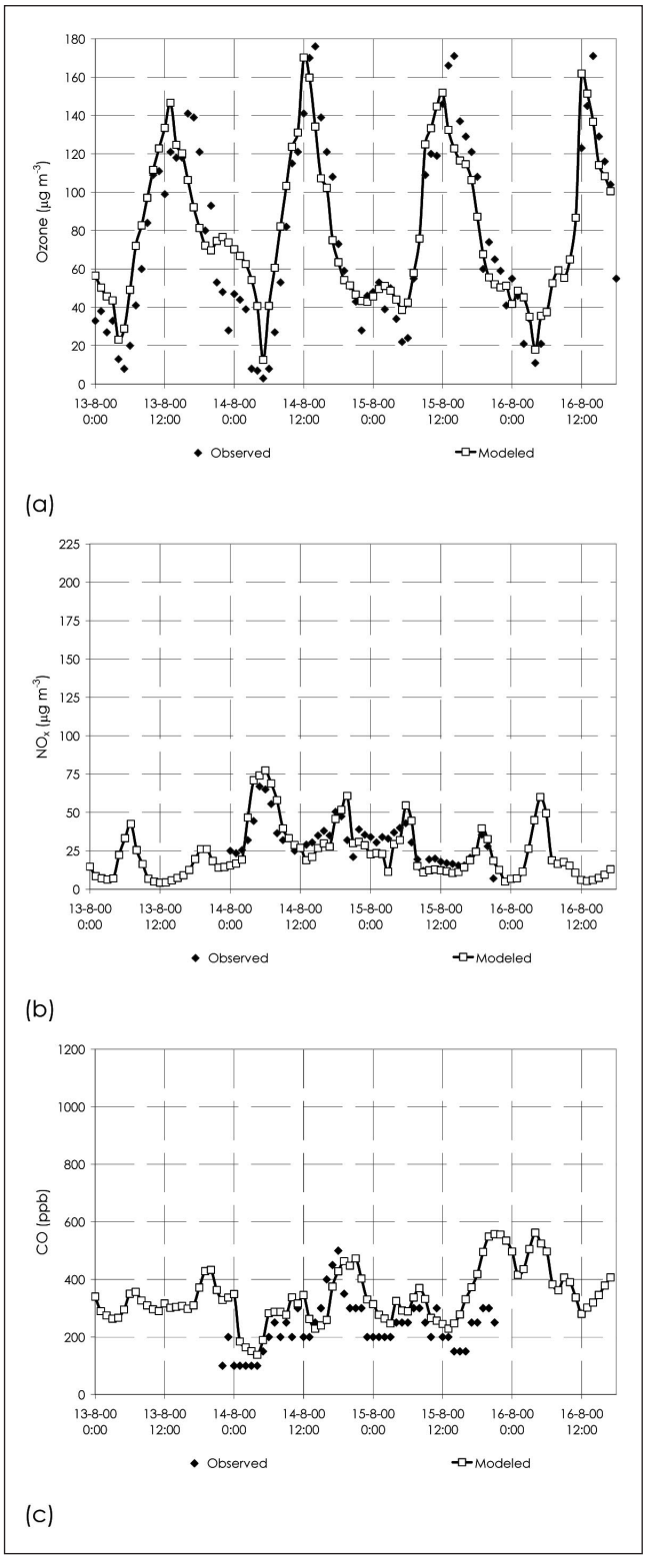

Figure 9. Time series for (a) ozone, (b) NO_x, and (c) CO for observations (black diamonds) and simulations (solid line, white squares) in the area of Vic for 13–16 August, 2000.

(–3.8 and –11.7%). The MNGE increased from August 13 until August 16 (16.8 to 26.7%), mainly due to deviations in meteorological predictions that became larger with the time of simulation (Jiménez *et al.*, 2005b). The objective set in Directive 2002/3/EC (deviation of 50% for the 1-h averages) was also met for the entire period of study. With respect to categorical forecasting, statistical parameters indicated that the A (percent of forecasts that correctly predict an exceedance or non-exceedance) was around 90% for every day of simulation, with the performance decreasing by the end of the episode. CSI and the POD yield more accurate values when O_3 peaks are higher (and when the 120 μg m^{-3} threshold taken as reference was more frequently exceeded). The value of B (B<1 for all simulations) indicated that exceedances are generally underpredicted, which is consistent with the MNBE value obtained for discrete evaluations. Lastly, the false-alarm ratio (FAR) was higher for the first and last day of the simulations (around 68%), because of both the possible influence of initialization during the first moments of simulation, which can be high for the sum of reservoir species for O_3 (Berge *et al.*, 2001), and the errors attributable to the meteorology, which accumulate over the period and perturb through the forecasts.

Other statistical parameters for ozone and its precursors (NO_x and CO)

Table 4 shows the results of the evaluation of MM5-EMI-CAT2000-CMAQ with different statistical parameters for O_3, CO, and NO_x compared to ambient data. Evaluation against 1649 measurements was performed in the case of O_3. The results show an *r* of 0.74 between the simulations and the ambient data. The MB (1.0 μg m^{-3}) indicated a tendency to overpredict the values. The RMSE was also low for regional simulations (13.4 μg m^{-3}). As noted by Russell and Dennis (2000), current air-quality models show a pervasive tendency towards underprediction of precursors (-20 to –50%). In the case of NO_x, –9.2% was obtained for NMB, and 6.1% for MNBE. The *r* between the observed and predicted NO_x concentrations at 48 stations was 0.75. The RMSE was 35.4 μg m^{-}

Table 4. Statistical evaluation of photochemical pollutants (O3, NOx, and CO) in the northeastern Iberian Peninsula during the episode of 13–16 August, 2000.

Ozone				
Observations	*Simulated*			
Mean (μg m^{-3})	63.6	64.8	N	1649
SD (μg m^{-3})	37.4	31.4	Coefficient of correlation (R)	0.74
CV (%)	58.7%	48.6%	MB (μg m^{-3})	1.04
Max (μg m^{-3})	189	188	MNBE (%)	37.9%
95th (μg m^{-3})	123	114	MFB (%)	5.6%
75th (μg m^{-3})	92	84	MAGE (μg m^{-3})	9.8
50th (μg m^{-3})	61	67	MNGE (%)	64.1%
25th (μg m^{-3})	33	42	NME (%)	30.8%
5th (μg m^{-3})	9	10	NMB (%)	1.7%
Min (μg m^{-3})	1	0	RMSE (μg m^{-3})	13.4
Nitrogen oxides				
Observations	*Simulated*			
Mean (μg m^{-3})	68.0	61.8	N	907
SD (μg m^{-3})	52.0	59.0	Coefficient of correlation (R)	0.75
CV (%)	76.4%	95.6%	MB (μg m^{-3})	-5.44
Max (μg m^{-3})	279	283	MNBE (%)	6.1%
95th (μg m^{-3})	149	165	MFB (%)	-23.8%
75th (μg m^{-3})	79	73	MAGE (μg m^{-3})	26.5
50th (μg m^{-3})	48	38	MNGE (%)	62.7%
25th (μg m^{-3})	28	17	NME (%)	44.4%
5th (μg m^{-3})	9	4	NMB (%)	-9.2%
Min (μg m^{-3})	3	1	RMSE (μg m^{-3})	35.4
Carbon monoxide				
Observations	*Simulated*			
Mean (μg m^{-3})	238.4	218.9	N	907
SD (μg m^{-3})	198.4	170.2	Coefficient of correlation (R)	0.74
CV (%)	83.2%	77.8%	MB (μg m^{-3})	-13.44
Max (μg m^{-3})	1150	1154	MNBE (%)	7.0%
95th (μg m^{-3})	700	600	MFB (%)	-2.7%
75th (μg m^{-3})	225	260	MAGE (μg m^{-3})	62.9
50th (μg m^{-3})	175	165	MNGE (%)	30.3%
25th (μg m^{-3})	100	110	NME (%)	38.4%
5th (μg m^{-3})	100	92	NMB (%)	-8.2%
Min (μg m^{-3})	50	69	RMSE (μg m^{-3})	104.1

^{3} for the regional model for NO_x predictions in the domain of the NWMB. In the case of CO, the *r* between the observed and predicted concentrations for the 907 observation values during this episode was 0.74, hence correlating worse than O_3 and NO_x in the study domain. The MB was –13.4 μg m^{-3} (MNBE of 7.0%), and the RMSE 104.1 μg m^{-3}. Summarizing, simulation with the CMAQ underestimated the maximum O_3, CO, and NO_x levels with respect to ambient data, since the grid resolution highly influenced the formation and loss processes of pollutants (especially photochemistry and vertical transport). Hence, the average volume defined by the model's horizontal grid spacing must be sufficiently small to allow the air quality to be reproduced accurately (Jiménez *et al.*, 2005b).

Conclusions

The methodology of photochemical modeling developed here by combining suitable models appears useful to investigate the cycles of air pollutants in the NWMB, accounting for large-scale processes as well as local orographical and land-sea breeze circulations,. This approach helps in understanding the relative importance of coupled processes involved during air pollution episodes, in particular for this area.

The models were evaluated against ambient data from 48 air-quality stations in the NWMB (Catalonia). The objective set in Directive 2002/3/EC was met for the entire period of study for MM5-EMICAT2000-CMAQ. The models also met the objectives of USEPA and European Directive 2002/3/EC for prediction of the levels of this pollutant during the episode.

With respect to the origin of the high levels of photochemical pollutants and their dynamics over the NWMB, the main processes that take place in the troposphere of the NWMB may be summarized as:

1. The distinctive episode of 13–16 August, 2000, which was chosen for an analysis of the processes over the NWMB, was characterized by a weak synoptic forcing, so that mesoscale phenomena, induced by the particular geography of the region, were dominant. The air pollution in the lower troposphere had a local origin and was associated mainly with recirculation processes.
2. During the episode, a strong land-sea breeze regime was established along the entire domain. Circulation cells up to 2 km in height, thus strongly extending over the mixing height (800 m), developed in the morning hours. The strength of the sea breeze, reinforced positively by the anabatic winds over the complex orography of the eastern Iberian coast, give rise to the vertical injection and layering of air pollutants. As the land-sea breeze front advanced inland, reaching the mountain ranges, orographical transport and mechanical recirculations of air pollutants occurred in the coastal mountains (~500 m). During the afternoon, the breeze reached the second mountain chain, reinforced by anabatic winds, producing upward motions up to 1.5–2 km in altitude. In the evening (20.00 UTC), the photochemical activity ceased, the land-see breeze regime lost intensity, and coastal winds weakened, producing drainage of pollutants towards the coast through the river valleys. At night, O_3 concentrations were further reduced as a consequence of titration by fresh NO emissions.
3. At an altitude of 0.5–1.5 km, air masses arriving in the NWMB had their origin near the southeastern Iberian coast. An O_3 reservoir layer at 1.5 km developed during the night over the Mediterranean Sea, with ozone concentrations in excess of 125 μg m^{-3}. The high-pressure area over the Mediterranean Sea was associated with anticyclonic circulation; therefore, air pollutants were transported inland on the following day during the development of the land-sea breeze cycle.
4. The intense surface heating promoted development of the ITL over the central Iberian Peninsula. It forced the convergence of surface winds from the coastal areas towards the central plateau over which convection transported polluted air masses into the middle troposphere. The northwesterly winds transported pollutants in a stratified layer at an altitude of 3.5 km towards the NWMB, where they further subsided and were incorporated into the land-sea breeze circulations.

In order to carry out high-resolution simulations (1-2 km and 1 h) and the application of third-generation air-quality models, high-performance computational resources are essential. In this framework, the existence of MareNostrum (at the Barcelona Supercomputing Center) is a key factor in successfully evaluating the problems caused by air pollutants, especially for those areas with a very complex topography and a high level of variability of the land cover.

Acknowledgments

This project was developed thanks to the IMMPACTE project funded by the Government of Catalonia in a special initiative of the Catalan Environmental Research Programme. This work was also developed under the research contract REN2003-09753-C02 of the Spanish Ministry of Science and Technology. Dr. Jos Lelieveld, from the Max Planck Institute for Chemistry (Mainz, Germany), is also thanked for his useful comments. Air-quality station data and information about industrial emissions were provided by the Environmental Department of the Government of Catalonia (Spain).

References

[1] Baldasano, J.M., Cremades, L., Soriano, C., 1994. Circulation of air pollutants over the Barcelona geographical area in summer. Proceedings of Sixth European Symposium Physic-Chemical Behavior of Atmospheric Pollutants. Varese (Italy), 18-22 October, 1993. Report EUR 15609/1 EN: 474-479.

[2] Berge, E., Huang, H.-C., Chang, J., Liu, T.-H., 2001. A

study of the importance of initial conditions for photochemical oxidant modeling. Journal of Geophysical Research, 106(D1), 1346-1363.

[3] Byun, D.W., Ching, J.K.S. (Eds.), 1999. Science algorithms of the EPA Models-3 Community Multiscale Air Quality (CMAQ) Modeling System. EPA Report N. EPA-600/R-99/030, Office of Research and Development. U.S. Environmental Protection Agency, Washington, DC.

[4] Dudhia, J., 1993. A nonhydrostatic version of the Penn State/NCAR mesoscale model: Validation tests and simulation of an Atlantic cyclone and cold front. Monthly Weather Review, 121, 1493–1513.

[5] Dueñas, C., Fernández, M.C., Cañete, S., Carretero, J., Liger, E., 2002. Assessment of ozone variations and meteorological effects in an urban area in the Mediterranean coast. The Science of the Total Environment, 299, 97-113.

[6] Gangoiti, G., Millán, M.M., Salvador, R., Mantilla, E., 2001. Long-range transport and re-circulation of pollutants in the western Mediterranean during the project regional cycles of air pollution in the west–central Mediterranean area. Atmospheric Environment, 35, 6267-6276.

[7] Gery, M.W., Whitten, G.Z., Killus, J.P., Dodge, M.C., 1989. A photochemical kinetics mechanism for urban and regional scale computer modeling. Journal of Geophysical Research, 94 (D10), 12925-12956.

[8] Hauglustaine, D.A., Brasseur, G.P., 2001. Evolution of tropospheric ozone under anthropogenic activities and associated radiative forcing on climate. Journal of Geophysical Research, 106, 32337-32360.

[9] Hogrefe, C., Rao, S.T., Kasibhatla, P., Hao, W., Sistla, G., Mathur, R., McHenry, J., 2001. Evaluating the performance of regional-scale photochemical modeling systems: Part II – ozone predictions. Atmospheric Environment, 35, 4175-4188.

[10] Kang, D., Eder, B.K., Schere, K.L., 2003. The evaluation of regional-scale air quality models as part of NOAA's air quality forecasting pilot program, in: 26th NATO International Technical Meeting on Air Pollution Modeling and its Application, Istanbul, Turkey, 404-411.

[11] Kang, D., Eder, B.K., Mathur, R., Yu, S., Schere, K.L., 2004. An operational evaluation of the ETA-CMAQ air quality forecast model, in: 27th NATO International Technical Meeting on Air Pollution Modeling and its Application, Banff, Canada, 233-240.

[12] Jiménez, P., Dabdub, D., Baldasano, J.M., 2003. Comparison of photochemical mechanisms for air quality modeling. Atmospheric Environment, 37, 4179-4194.

[13] Jiménez, P., Parra, R., Baldasano, J.M., 2005a. Modeling the ozone weekend effect in very complex terrains: a case study in the northeastern Iberian Peninsula. Atmospheric Environment, 39, 429-444.

[14] Jiménez, P., Jorba, O., Parra, R., Baldasano, J.M., 2005b. Influence of high-model grid resolution on photochemical modeling in very complex terrains. International Journal of Environment and Pollution, 24, Nos. 1/2/3/4, 180-200.

[15] Jorba, O., Pérez, C., Rocadenbosch, F., Baldasano, J.M., 2004. Cluster Analysis of 4-Day Back Trajectories Arriving in the Barcelona Area (Spain) from 1997 to 2002. Journal of Applied Meteorology, 43, 6, 887-901.

[16] Lawrence, M.G., Crutzen, P.J., Rasch, P.J., Eaton, B.E., Mahowald, N.M., 1999. A model for studies of tropospheric photochemistry: description, global distributions and evaluation. Journal of Geophysical Research, 104, 26245-26277.

[17] Lelieveld, J., Berresheim H., Borrmann, S., Crutzen, P.J., Dentener, F.J., Fischer, H., Feichter, J., Flatau, P.J., Heland, J., Holzinger, R., Korrmann, R., Lawrence, M.G., Levin, Z., Markowicz, K.M., Mihalopoulos, N., Minikin, A., Ramanathan, V., de Reus, M., Roelofs, G.J., Scheeren, H.A., Sciare, J., Schlager, H., Schultz, M., Siegmund, P., Steil, B., Stepahanou, E.G., Stier, P., Traub, M., Warneke, C., Williams, J., Zieris, H., 2002. Global air pollution crossroads over the Mediterranean. Science, 298, 794-799.

[18] Millán, M.M., Salvador, R., Mantilla, E., Artíñano, B., 1996. Meteorology and photochemical air pollution in southern Europe: Experimental results from EC research projects. Atmospheric Environment, 30, 1909-1924.

[19] Millán, M.M., Salvador, R., Mantilla, E., 1997. Photooxidant dynamics in the Mediterranean basin in summer: Results from European research projects. Journal of Geophysical Research, 102 (D7), 8811-8823.

[20] Millán, M.M., Mantilla, E., Salvador, R., Carratala, A., Sanz, M.J., Alonso, L., Gangoiti, G., Navazo, M., 2000. Ozone cycles in the western Mediterranean basin: interpretation of monitoring data in complex coastal terrain. Journal of Applied Meteorology, 4, 487-507.

[21] Ntziachristos, L., Samaras, Z., 2000. COPERTIII Computer programme to calculate emissions from road transport. Methodology and emission factors (Version 2.1). European Environment Agency. Technical report No 49.

[22] Parra, R., Jiménez, P., Baldasano, J.M., 2006. Development of the high spatial resolution EMICAT2000 emission model for air pollutants from the north-eastern Iberian Peninsula (Catalonia, Spain). Environmental Pollution 140, 200-219.

[23] Pérez, C., Sicard, M., Jorba, O., Comerón, A., Baldasano, J.M., 2004. Summertime re-circulations of air pollutants over the north-eastern Iberian coast observed from systematic EARLINET lidar measurements in Barcelona. Atmospheric Environment, 38, 3983-4000.

[24] Ribas, A., Peñuelas, J., 2004. Temporal patterns of surface ozone levels in different habitats of the North Western Mediterranean basin. Atmospheric Environment, 38, 985-992.

[25] Russell, A., Dennis, R., 2000. NARSTO critical review of photochemical models and modeling. Atmospheric Environment 34, 2283-2324.

[26] Sicard, M., Pérez, C., Rocadenbosch, F., Baldasano, J.M., García-Vizcaino, D., 2006. Mixed-layer depth determination in the Barcelona coastal area from regular lidar measurements: methods, results and limitations. Boundary-Layer Meteorology, In Press.

[27] Tesche, T.W., Lurmann, F.L., Roth, P.M., Georgopoulos, P., Seinfeld, J.H., Cass, G., 1990. Improvement of Procedures for Evaluating Photochemical Models. Report to California Air Resources Board for Contract No. A832-103. Alpine Geophysics, LLC, Crested Butte, Colorado.

[28] Toll, I., Baldasano, J.M., 2000. Modeling of photochemical air pollution in the Barcelona area with highly disaggregated anthropogenic and biogenic emissions. Atmospheric Environment, 34, 19, 3060-3084.

[29] US EPA, 1991. Guideline for Regulatory Application of the Urban Airshed Model. US EPA Report No. EPA-450/4-91-013. Office of Air and Radiation, Office of Air Quality Planning and Standards, Technical Support Division. Research Triangle Park, North Carolina, US.

[30] Ziomas, I.C., Gryning, S.E., Borsteing, R.D., 1998. The Mediterranean campaign of photochemical tracers-transport and chemical evolution (MEDCAPHOT-TRACE). Atmospheric Environment, 32, 2043-2326.

About the author